Electromagnetically induced transparency and optical switching in a rubidium cascade system

Jason Clarke, Hongxin Chen, and William A. van Wijngaarden

Electromagnetically induced transparency is observed in a mismatched-wavelength cascade system with a room-temperature rubidium vapor cell. A cw probe laser beam monitors the $5S_{1/2} \rightarrow 5P_{3/2}$ transition while another cw laser couples the $5P_{3/2}$ state to a higher excited state. The ratio of the observed Rabi frequencies for coupling to the $5P_{3/2} \rightarrow 8D_{3/2,5/2}$ transitions agrees well with that predicted by use of the transition oscillator strengths. Optical switching is demonstrated with an 80-mW coupling laser beam modulated up to 1 MHz.

OCIS codes: 270.1670, 020.4900, 060.1810, 060.4080, 300.6210.

1. Introduction

Recently there has been a surge of interest in electromagnetically induced transparency (EIT) in three- and multiple-level systems.[1–6] EIT is a quantum interference effect that occurs when a weak probe light field, in resonance with an atomic transition, propagates through a medium with reduced absorption that is due to the presence of a strong coupling light field on a linked transition. The three energy levels involved can be in cascade, Λ, and V configurations.[7] The first observation of EIT was made with high-power pulsed lasers interacting with a strontium vapor in a Λ system.[8,9] A number of sub-Doppler cw EIT experiments have been carried out with vapor cells,[10–18] atomic beams,[19] laser-cooled atoms,[20–27] and even Bose condensates.[28,29] The latter were used to demonstrate ultraslow photon velocities. Some research has also been done on solids.[30] EIT and other coherence effects in three- and four-level systems have applications in nonlinear optics such as enhancement of four-wave mixing[31,32] and lasing without population inversion.[18,19] Most EIT experiments have been performed with a so-called matched system in which the probe and coupling laser wavelengths are nearly equal. A few experiments have been used to study mismatched systems with the goal of achieving inversionless lasing on high-frequency transitions.[15,17] EIT has also been proposed for developing optical switches and wavelength converters for telecommunications.[33,34] Shepherd *et al.*[15] studied EIT in a 2-cm-long rubidium cell heated to 50 °C. The coupling laser was resonant with a transition from the $5P_{3/2}$ to one of the $5D_{5/2}$, $7D_{5/2}$, or $7S_{1/2}$ states while the probe laser monitored the $5S_{1/2} \rightarrow 5P_{3/2}$ transition. The EIT signal was found to depend strongly on the coupling transition wavelength.

We report observations of EIT in a mismatched system that included a room-temperature rubidium vapor. A low-power diode laser is used to monitor the $5S_{1/2} \rightarrow 5P_{3/2}$ transition while a higher-power ring dye laser couples the $5P_{3/2}$ state to either the $8D_{3/2}$, $8D_{5/2}$, or $10S_{1/2}$ state. Finally, an optical switch whereby the intensity modulation of the coupling laser beam induces modulation of the probe laser is demonstrated at a rate of up to 1 MHz.

2. Experimental Arrangement

The apparatus is illustrated in Fig. 1. Rubidium atoms were contained in a vapor cell with a diameter of 2.5 cm and a length of 5 cm. This Pyrex cell was baked overnight at a temperature of 300 °C to remove impurities while simultaneously attached to a vacuum system and pumped with a diffusion pump and a liquid-nitrogen trap to a pressure of 2×10^{-7} Torr. The oven was then turned off, and rubidium was distilled into the cell. Most of our measurements were taken at room temperature where the density of rubidium is 10^9 atoms/cm^3.[35]

An external cavity-grating-controlled laser diode (TuiOptics Model DL 100) was used as the probe laser. It has a linewidth of less than 1 MHz and produces 30 mW of light at 780 nm. The diode laser can be

The authors are with the Department of Physics, Petrie Building, York University, 4700 Keele Street, Toronto, Ontario M3J 1P3, Canada. The e-mail address for W. A. van Wijngaarden is wvw@yorku.ca.

Received 3 August 2000; revised manuscript received 2 January 2001.

0003-6935/01/122047-05$15.00/0

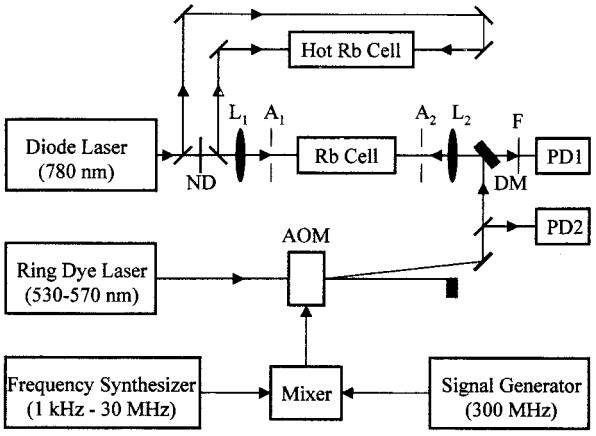

Fig. 1. Apparatus; see text for description.

scanned over 10 GHz without mode hops. The laser beam was carefully collimated by use of lenses. An aperture was used to create a nearly spatially uniform probe beam with a diameter of 2 mm, and a neutral-density filter (ND) reduced the power to ~10 μW. The low-power probe beam was used to avoid optical pumping effects, and its absorption through the room-temperature cell could be readily measured. The diode laser frequency was monitored with saturation spectroscopy.

The coupling laser beam was generated by a ring dye laser (Coherent Model 699–21) that was pumped by an argon-ion laser. The ring dye laser has a linewidth of less than 1 MHz and generates ~300 mW in the wavelength range of 530–570 nm with Pyromethene 556 laser dye. The ring dye laser coupled the $5P_{3/2}$ state to higher excited states as shown in Fig. 2. The dye laser frequency was monitored with a rubidium cell maintained at a temperature of 80 °C. Rubidium atoms in this hot cell were excited with several milliwatts of light generated by the diode laser and ~40 mW of dye laser light. The high temperature of the cell enabled fluorescence produced by the radiative decay of the high lying states back to the $5P_{3/2}$ to be visible when the dye laser excited the atoms. In contrast, no such fluorescence could be seen from the room-temperature rubidium cell used to observe EIT.

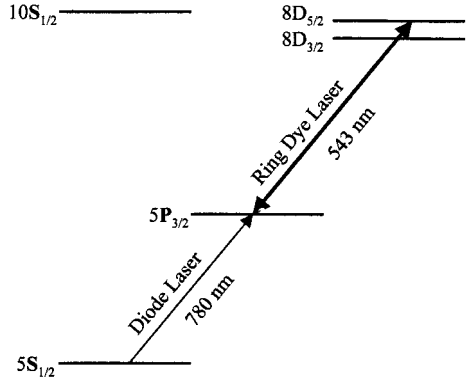

Fig. 2. Rubidium energy levels used in experiment. The cw diode probe laser monitors the $5S_{1/2} \rightarrow 5P_{3/2}$ transition, whereas the cw dye laser coupled the $5P_{3/2}$ state to one of the $10S_{1/2}$, $8D_{3/2}$, or $8D_{5/2}$ excited states.

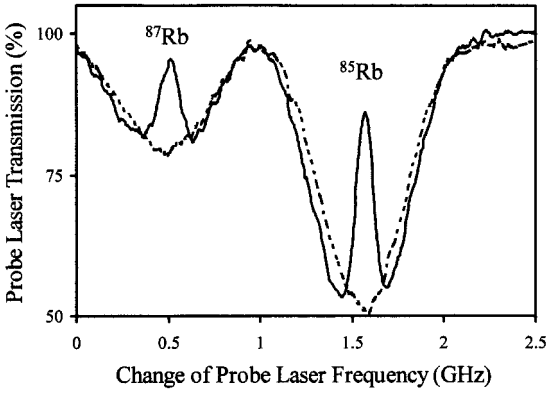

Fig. 3. Probe laser transmission versus change of probe laser frequency. The dashed curve was taken by means of scanning the diode laser across the D_2 line of ^{85}Rb and ^{87}Rb without any coupling laser present. The solid curve was taken with 280 mW of dye laser light coupled to the $5P_{3/2} \rightarrow 8D_{5/2}$ transition.

The diode and dye laser beams were focused with lenses of 10-cm focal length (L_1 and L_2, respectively). The laser beams next passed through apertures A_1 (diameter, 0.5 mm) and A_2 (diameter, 2 mm), respectively. The diode laser beam waist at the focus was 50 μm , whereas that of the dye laser beam was 60 μm. The resulting power density of the coupling laser was estimated to be 1×10^4 W/cm^2. The overlap of the two laser foci was achieved by optimization of the EIT signal. Both probe and coupling laser beams were linearly polarized in the vertical direction.

The laser beams were monitored with two photodiodes (ThorLabs Model PDA55) that have a detection bandwidth of 10 MHz. A filter F blocked scattered dye laser light. Detector PD1 observed the diode laser beam transmitted through the rubidium cell and through a dielectric mirror DM that reflected visible wavelengths but transmitted the infrared diode laser beam. Part of the dye laser beam incident on the cell was monitored by the second photodiode, PD2. Both photodiode signals were sent to a digitizing oscilloscope (Tektronix Model TDS 3052) having a bandwidth of 500 MHz.

3. Results

We observed the EIT signal by measuring the diode laser power transmitted through the rubidium cell as the diode laser frequency was scanned across the $5S_{1/2} \rightarrow 5P_{3/2}$ resonance. The dashed curve in Fig. 3 shows two dips corresponding to absorption of the diode laser by ^{87}Rb and ^{85}Rb in the absence of the coupling laser. The Doppler width (FWHM intensity) is shown to be 530 MHz. The solid curve was taken with 280 mW of dye laser light resonant with the $5P_{3/2} \rightarrow 8D_{5/2}$ transition. The two peaks at the centers of the absorption dips are the EIT signals. For the ^{87}Rb peak, the diode laser beam transmission through the cell increased from 80% to nearly 100%, whereas for ^{85}Rb the transmission increased from 50% to ~88%.

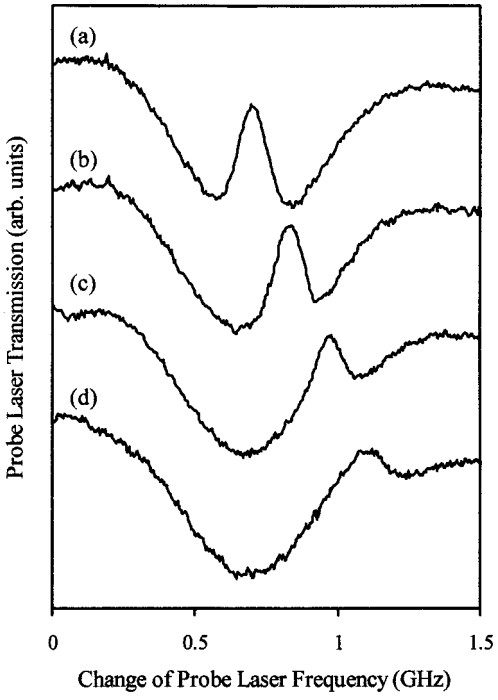

Fig. 4. Effect of detuning the coupling laser on the EIT signal. The coupling laser frequency was detuned from the $5P_{3/2} \rightarrow 8D_{5/2}$ transition of ^{85}Rb. Detuning the coupling laser is as follows: (a) 0 GHz, (b) 0.13 GHz, (c) 0.26 GHz, (d) 0.40 GHz. The dye laser power of 280 mW was the same for all four scans.

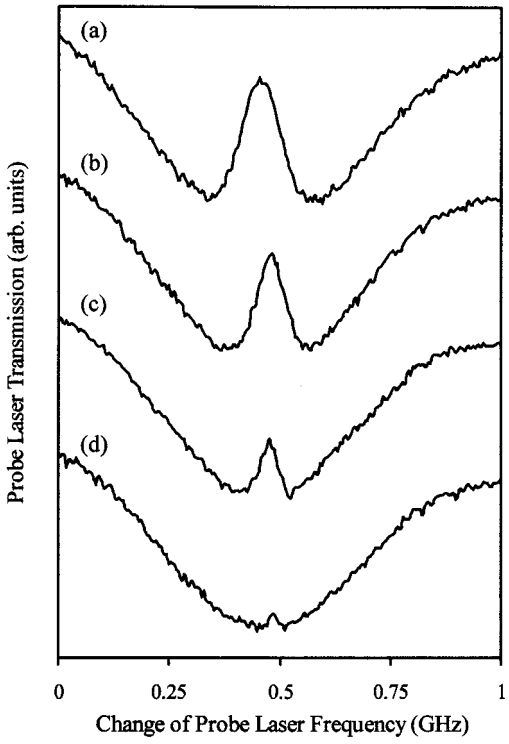

Fig. 5. Effect of coupling laser power on the EIT signal. The dye laser coupled to the $5P_{3/2} \rightarrow 8D_{5/2}$ transition of ^{85}Rb. The dye laser power varied from (a) 280 mW, (b) 80 mW, (c) 12 mW, and (d) 2 mW. All other experimental parameters were kept constant.

The dependence of the EIT signal with the detuning of the dye laser from the $5P_{3/2} \rightarrow 8D_{5/2}$ transition is shown in Fig. 4. The four scans were all taken with a dye laser beam power of 280 mW. The effect of the coupling laser is most evident when it is on resonance. The dependence of the coupling laser power on the EIT signal is shown in Fig. 5. The coupling laser power was varied with calibrated neutral-density filters. The EIT signal was still visible with a 2-mW coupling laser beam.

Figure 6 shows the dependence of the EIT signal when the coupling laser couples to different excited states. The three scans were taken with the same coupling laser power of 280 mW. Clearly, the EIT signal depends strongly on the coupling transition. The width of the EIT peak is determined by the Rabi frequency Ω[17] given by

$$\Omega = e\langle r\rangle E/\hbar, \tag{1}$$

where e is the electron charge, $\langle r\rangle$ is the expectation of the electron position for the coupling transition, E is the laser electric field, and $\hbar$ is Planck's constant. Alternatively, the Rabi frequency can be expressed as

$$\Omega \propto (KfI)^{1/2}, \tag{2}$$

where f is the absorption oscillator strength for the coupling transition, I is the laser intensity, and K is a constant that depends on the transition.[15] From Fig. 6 the Rabi frequencies for coupling the $5P_{3/2}$ state to the $8D_{5/2}$ and $8D_{3/2}$ states are found to be 188 and 60 MHz, respectively. The observed transparencies are in qualitative agreement with the EIT model presented in Ref. 15. Moreover, the ratio of these Rabi frequencies, $188/60 = 3.1$, agrees well with the result of 3.0 found by taking the square root of the absorption oscillator strengths for the $5P_{3/2} \rightarrow 8D_{5/2}$ and $5P_{3/2} \rightarrow 8D_{3/2}$ transitions, which have values of 1.56×10^{-2} and 1.75×10^{-3}, respectively.[36,37] This gives important confirmation of the theoretical relative oscillator strength.

4. Optical Switching

Optical switching was done with an acousto-optic modulator (AOM) (Brimrose Model TEF 27–10) to modulate the intensity of the dye laser beam as follows. The AOM generated a laser beam shifted by 300 MHz and with a power of 80 mW. The frequency-shifted and frequency-unshifted laser beams were spatially separated by a few milliradians. The signal to the AOM consisted of a 300-MHz sine wave produced by a frequency synthesizer (Hewlett-Packard Model 8645A). This signal was mixed with a square wave having a frequency of up to 1 MHz by a mixer (Mini-Circuits Model 15542), amplified to a power of 1 W and sent to the AOM.

The solid curves in Fig. 7 represent the intensity of the coupling laser beam. The coupling laser intensity could be completely switched off at modulation frequencies of 10 and 100 kHz. At 1 MHz the minimum coupling laser intensity was $\sim 1/3$ its maximum value.

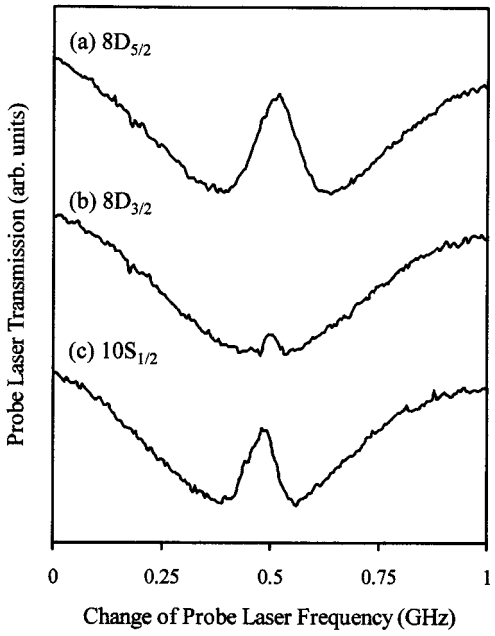

Fig. 6. Effect of excited-state coupling on the EIT signal. The upper state of ^{85}Rb coupled by the dye laser was (a) $8D_{5/2}$, (b) $8D_{3/2}$, (c) $10S_{1/2}$. The dye laser power for all three scans was 280 mW.

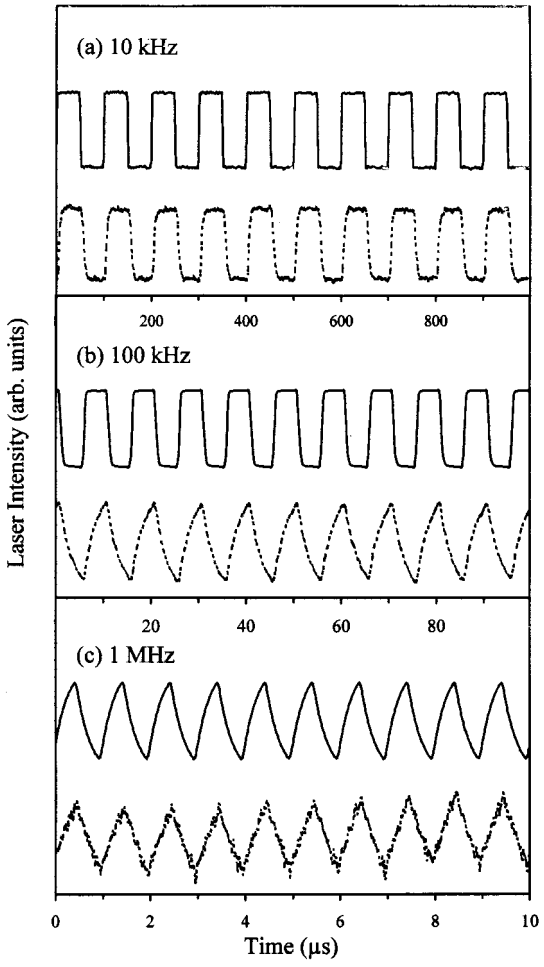

Fig. 7. Optical switching of the probe laser by the coupling laser. Solid curve, intensity of the coupling laser; dashed curve, intensity of the probe laser. The observed increase in the probe laser transmission that is due to the frequency-modulated coupling laser beam was (a) 25% at 10 kHz, (b) 17% at 100 kHz, and (c) 3% at 1 MHz. The signals are discussed in the text.

The data in Fig. 7 were all taken with a room-temperature cell. The coupling laser was centered on the $5P_{3/2} \rightarrow 8D_{5/2}$ transition of ^{85}Rb, whereas the diode probe laser frequency was fixed on the center of the $5S_{1/2} \rightarrow 5P_{3/2}$ transition of ^{85}Rb. This was done to maximize the modulation induced in the probe laser. The probe laser modulation corresponded exactly to that of the coupling laser for modulation frequencies of 10 kHz or less. This is illustrated in Fig. 7(a) where the transmission of the diode laser beam through the rubidium cell increased from 50% to 75%, because of the coupling laser beam. When the cell was heated to 60 °C, the coupling laser beam increased the probe laser beam transmission from less than 1% to 60%.

For a modulation frequency of 100 kHz as shown in Fig. 7(b) the probe laser beam did not respond as quickly as the coupling laser beam. The response time depends on the coupling laser power,[22] which in our case was only 80 mW. The coupling laser beam caused the probe laser beam transmission to increase by 25% at a modulation frequency of 10 kHz [see Fig. 7(a)], 17% at 100 kHz [see Fig. 7(b)], and 3% at 1 MHz [see Fig. 7(c)].

4. Conclusions

There is great interest in developing a rapid and practical optical switch for processing telecommunication signals. EIT has the advantage of being relatively simple, requiring only a coupling laser focused into a room-temperature vapor cell. The time response is determined by the coupling laser intensity. Hence, for a given optical arrangement, higher switching speeds require larger coupling laser powers. It is noteworthy that laser power has been increased by a factor of 1000 by passage of a diode laser beam into an optical cavity constructed with high-finesse mirrors.[38] The time response of such a cavity-based switch would, of course, depend on the cavity's length and finesse.

The ultimate limiting time response of a switch is the time it takes for the laser beam to traverse the cell. For a 5-cm-long cell this is 0.17 ns. This temporal limit cannot be circumvented regardless of the coupling laser intensity. A faster response can be obtained by means of replacing the cell with a sample of laser-cooled atoms. Laser-cooled atom clouds are routinely generated with a size of less than 1 mm. Doppler broadening is negligible at temperatures of less than 1 mK. These advantages for EIT signals have been exploited with cold alkali atoms.[20,24,28]

In this experiment an intensity-modulated coupling laser operating at a visible wavelength switched an infrared laser. The reverse can also be done. It may be interesting to consider atoms such as barium, which has several D states below its first excited P state. The barium $(6s)^2\ ^1S_0 \rightarrow 6s6p\ ^1P_1$ transition occurs at 554 nm, whereas the $6s6p\ ^1P_1 \rightarrow (6s6d)\ ^{1,3}D$ transi-

tions occur at 1.1 and 1.5 μm. The latter wavelength is especially important for telecommunications. Hence optical switching with simple atomic systems complements research done in semiconductor materials.

The authors thank A. Kumarakrishnan for the loan of a mixer and T. Scholl for technical advice with the ring dye laser. We also acknowledge the support of the Natural Science and Engineering Research Council of Canada and the Canadian Institute for Photonic Innovations. J. Clarke is the recipient of a JDS Uniphase scholarship for graduate studies.

References and Note

1. S. E. Harris, "Electromagnetically induced transparency," Phys. Today **50,** 36–42 (1997).
2. J. P. Marangos, " Electromagnetically induced transparency," J. Mod. Opt. **45,** 471–503 (1998).
3. M. O. Scully and M. S. Zubairy, *Quantum Optics* (Cambridge U. Press, Cambridge, UK, 1997), Chap. 7.
4. O. Kacharovskaya, "Amplification and lasing without inversion," Phys. Rep. **219,** 175–190 (1992).
5. M. O. Scully, "From lasers and masers to phaseonium and phasers," Phys. Rep. **219,** 191–201 (1992).
6. P. Mandel, "Lasing without inversion: a useful concept?" Contemp. Phys. **34,** 235–246 (1993).
7. D. J. Fulton, S. Shepherd, R. R. Moseley, B. D. Sinclair, and M. H. Dunn, "Continuous-wave electromagnetically induced transparency: a comparison of V, lambda, and cascade systems," Phys. Rev. A **52,** 2302–2311 (1995).
8. K. J. Boller, A. Imamoglu, and S. E. Harris, "Observation of electromagnetically induced transparency," Phys. Rev. Lett. **66,** 2593–2596 (1991).
9. J. E. Field, K. H. Hahn, and S. E. Harris, "Observation of electromagnetically induced transparency in collisionally broadened lead vapor," Phys. Rev. Lett. **67,** 3062–3065 (1991).
10. M. Xiao, Y. Li, S. Jin, and J. Gea-Banacloche, "Measurement of dispersive properties of electromagnetically induced transparency in rubidium atoms," Phys. Rev. Lett. **74,** 666–669 (1995).
11. J. Gea-Banacloche, Y. Li, and S. J. M. Xiao, "Electromagnetically induced transparency in ladder-type inhomogeneously broadened media: theory and experiment," Phys. Rev. A **51,** 576–584 (1995).
12. Y. Li and M. Xiao, "Electromagnetically induced transparency in a three-level lambda system in rubidium atoms," Phys. Rev. A **51,** R2703–2706 (1995).
13. Y. Li and M. Xiao, "Observation of quantum interference between dressed states in an electromagnetically induced transparency," Phys. Rev. A **51,** 4959–4962 (1995).
14. R. R. Moseley, S. Shepherd, D. J. Fulton, B. D. Sinclair, and M. H. Dunn, "Two-photon effects in continuous-wave electromagnetically-induced transparency," Opt. Commun. **119,** 61–68 (1995).
15. S. Shepherd, D. J. Fulton, and M. H. Dunn, "Wavelength dependence of coherently induced transparency in a Doppler-broadened cascade medium," Phys. Rev. A **54,** 5394–5399 (1996).
16. J. R. Boon, E. Zekou, D. McGloin, and M. H. Dunn, "Comparison of wavelength dependence in cascade-, lambda-, and Vee-type schemes for electromagnetically induced transparency," Phys. Rev. A **59,** 4675–4684 (1999).
17. J. R. Boon, E. Zekou, D. J. Fulton, and M. H. Dunn, "Experimental observation of a coherently induced transparency on a blue probe in a Doppler-broadened mismatched V-type system," Phys. Rev. A. **57,** 1323–1328 (1998).
18. A. S. Zibrov, M. D. Lukin, D. E. Nikonov, L. Hollberg, M. O. Scully, V. L. Velichansky, and H. G. Robinson, "Experimental demonstration of laser oscillation without population inversion via quantum interference in Rb," Phys. Rev. Lett. **75,** 1499–1502 (1995).
19. G. G. Padmabandu, G. R. Welch, I. N. Shubin, E. S. Fry, D. E. Nikonov, M. D. Lukin, and M. O. Scully, "Laser oscillation without population inversion in a sodium atomic beam," Phys. Rev. Lett. **76,** 2053–2056 (1996).
20. S. A. Hopkins, E. Usadi, H. X. Chen, and A. V. Durrant, "Electromagnetically induced transparency of laser-cooled rubidium in three-level lambda systems," Opt. Commun. **138,** 185–192 (1997).
21. A. V. Durrant, H. X. Chen, S. A. Hopkins, and J. A. Vaccaro, "Zeeman-coherence-induced transparency and gain inversion in laser-cooled rubidium," Opt. Commun. **151,** 136–146 (1998).
22. H. X. Chen, A. V. Durrant, J. P. Marangos, and J. A. Vaccaro, "Observation of transient electromagnetically induced transparency in a rubidium lambda system," Phys. Rev. A **58,** 1545–1548 (1998).
23. T. van der Veldt, J. F. Roch, P. Grelu, and P. Grangier, "Nonlinear absorption and dispersion of cold Rb-87 atoms," Opt. Commun. **137,** 420–426 (1997).
24. F. S. Cataliotti, C. Fort, T. W. Hansch, M. Inguscio, and M. Prevedelli, "Electromagnetically induced transparency in cold free atoms: test of a sum rule for nonlinear optics," Phys. Rev. A **56,** 2221–2224 (1997).
25. C. Fort. F. S. Cataliotti, M. Prevedelli, and M. Inguscio, "Temperature-selective trapping of atoms in a dark state by means of quantum interference," Opt. Lett. **22,** 1107–1109 (1997).
26. M. Mitsunaga and N. Imoto, "Observation of an electromagnetically induced grating in cold sodium atoms," Phys. Rev. A **59,** 4773–4776 (1999).
27. C. Fort, F. S. Cataliotti, T. W. Hansch, M. Inguscio, and M. Prevedelli, "Gain without inversion on the cesium D1 line," Opt. Commun. **139,** 31–34 (1997).
28. L. V. Hau, S. E. Harris, Z. Dutton, and C. H. Behroozi, "Light speed reduction to 17 metres per second in an ultracold atomic gas," Nature (London) **397,** 594–598 (1999).
29. S. E. Harris, L. V. Hau, "Nonlinear optics at low light levels," Phys. Rev. Lett. **82,** 4611–4614 (1999).
30. B. S. Ham, S. M. Shahriar and P. R. Hemmer, "Electromagnetically induced transparency over spectral hole-burning temperature in a rare-earth-doped solid," J. Opt. Soc. Am. B **16,** 801–804 (1999).
31. Y. Li and M. Xiao, "Enhancement of nondegenerate four-wave mixing based on electromagnetically induced transparency in rubidium atoms," Opt. Lett. **21,** 1064–1066 (1996).
32. J. C. Petch, C. H. Keitel, P. L. Knight, and J. P. Marangos, "Role of electromagnetically induced transparency in resonant four-wave-mixing schemes," Phys. Rev. A **53,** 543–561 (1996).
33. S. E. Harris and Y. Yamamoto, "Photon switching by quantum interference," Phys. Rev. Lett. **81,** 3611–3614 (1998).
34. H. Schmidt and R. J. Ram, "All-optical wavelength converter and switch based on electromagnetically induced transparency," Appl. Phys. Lett. **76,** 3173–3175 (2000).
35. $\mathrm{Log}_{10}[\mathrm{Rb}] = -4560/T + 30.98 - 2.45\,\mathrm{Log}_{10}\,T$ where T is in kelvins and [Rb], is in cm^{-3}. See C. J. Smithells, *Metals Reference Book* (Butterworth, London, UK, 1962).
36. D. R. Bates and A. Damgaard, "Calculation of the absolute strengths of spectral lines," Phil. Trans. Roy. Soc. **242,** 101–111 (1949).
37. W. A. van Wijngaarden, "Scalar and tensor polarizabilities of low lying S, D, F and G states in rubidium," J. Quant. Spectrosc. Radiat. Trans. **57,** 275–279 (1997).
38. C. E. Tanner, B. P. Masterson, and C. E. Wieman, "Atomic beam collimation using a laser diode with a self-locking power-buildup cavity," Opt. Lett. **13,** 357–359 (1988).